

## Research Article

**Assessment of Spatio-Temporal changes of Forest Cover using Remote Sensing techniques in Pavagadh Region, Gujarat State, India**Foram Jadeja<sup>1\*</sup> , Kauresh Vachhrajani<sup>2</sup> , Manik H. Kalubarme<sup>3</sup> <sup>1</sup> Department of Environmental Studies, Faculty of Science, The Maharaja Sayajirao University of Baroda, Gujarat, India<sup>2</sup> Department of Zoology, Faculty of Science, The Maharaja Sayajirao University of Baroda, Gujarat, India<sup>3</sup> Space Applications Centre, Indian Space Research Organization (ISRO), Ahmedabad, Gujarat, India\* Corresponding author: Foram Jadeja  
E-mail: foram.jadeja-envphd@msubaroda.ac.inReceived 17.08.2023  
Accepted 25.11.2023**How to cite:** Jadeja et al., (2023). Assessment of Spatio-Temporal changes of Forest Cover using Remote Sensing techniques in Pavagadh Region, Gujarat State, India. *International Journal of Environment and Geoinformatics (IJEGEO)*, 10(3): 039-047. doi. 10.30897/ijegeo.1344777**Abstract**

For effective forest management, it is essential to consider forest patterns and periodic changes in forest cover. Several spectral vegetation indices derived from multi-temporal Remote Sensing data are useful to track the changes over time. The major objective of this study was to monitor the changes in forest cover during the past three decades in the Pavagadh area of Panchmahal district, Gujarat State, India. Various indices like Normalized Difference Vegetation Index (NDVI), Land Surface Temperature (LST), and Urban Thermal Field Variance Index (UTFVI) with the Ecological Evaluation Index (EEI) were analyzed for assessment of Spatio-temporal changes in the forest cover. Multi-temporal Landsat-TM and OLI sensor data for the years 1991, 2001, 2011, and 2021 were utilized covering the study area. The Landsat-8, Thermal infrared sensor Band-10 data, and operational land imager Band-4 and Band-5 data were used in the estimation of LST. The results indicated that the total forest cover area has gradually increased from 1991 to 2021 and the total forest area has doubled during this period of 30 years. The LST distribution map illustrates that temperatures have risen primarily in the middle and western sections of the research area by almost 3-4 °C during 2021 as compared to 1991. The comparative study of NDVI and LST map brings out a significant fact that in the areas where moderate and dense forest cover is present, the LST was lower as compared to areas with poor vegetation cover. This indicates that there is an inverse relationship between forest cover distribution and LST. However, the Ecological evaluation index shows that the forest vegetation quality is gradually improving to normal conditions with the excellent category and UTFVI value (< 0) in reference to the year 1991.

**Keywords:** NDVI, Land Surface Temperature, UTFVI, Ecological evaluation index, Forest cover change**Introduction**

Forests are the ubiquitous terrestrial ecosystem and are distributed across the globe. They are vital to all of humanity because they provide a diverse range of resources and raw materials, help to regulate climate change, act as a hydrological flow modulator, are especially beneficial for carbon storage, and serve as a habitat for organisms. Environmental parameters, directly and indirectly, influence the growth and productivity of the forest through changes in temperature, precipitation, weather and others, which play an essential role in forest health. The technique of identifying differences in the condition of an object or phenomenon by examining it at different times is known as change detection (Yismaw, 2014). Changes in forest cover are a pervasive and rapid process influenced mostly by natural and artificial factors. For healthy forest management, it is necessary to understand the forest patterns and dynamic changes in forest cover. Remote sensing techniques and satellite-based data are immensely applicable and beneficial for change detection. It offers one of the most precise methods for determining the extent and pattern of variations in cover conditions over time (Forkuo, 2012).

**Vegetation Monitoring using Normalized Differential Vegetation Index (NDVI)**

Among the various methods, vegetation indices have proven to be reliable in monitoring vegetation change. The Normalized Differential Vegetation Index (NDVI) is a vital vegetation index that is generally used to assess the health of an area's vegetation. The NDVI concept is premised on the fact that healthy vegetation has low reflectance in the visible region of the Electromagnetic Spectrum (EMS) due to chlorophyll and other pigment absorption, and high reflectance in the Near-Infrared (NIR) due to internal reflectance by the green leaf's mesophyll spongy tissue (Nath, 2014; Esetlili et al., 2018). It helps to distinguish healthy vegetation from others. Using the NDVI technique, Nath B. (2014) quantified the forest cover changes of the Bandarban Hill Tracts regions, Bangladesh from the year 1989-2010 and categorized NDVI values based on statistics in the following manner i.e., no vegetation, less vegetation, less-moderate vegetation, moderated vegetation, dense vegetation and highly dense vegetation. Thus, he found that forest cover is declining at a rate of 0.74% each year. Similarly, Yismaw *et al.*, (2014) assessed the rate of forest cover change of 120 ha/year in Banja district, Ethiopia,

between 1973 and 2003. Likewise, Malik *et al.*, (2017) used NDVI to measure the forest cover change detection in district Baramulla, the Indian union territory of Jammu and Kashmir from the year 1980 to 2014, classified the NDVI values into four categories blank (< 0), sparse (0-0.2), moderate (0.2-0.4), dense(> 0.4) and observed that major change was detected from the dense forest to moderate forest and from sparse forest to blank forest, 138.59 km<sup>2</sup> and 167 km<sup>2</sup> respectively. According to Aburas *et al.*, (2015), the NDVI index is used as an essential indicator for detecting variations in land use and cover patterns. Using the same index, they discovered a declining trend in dense vegetation areas in Seremban, Malaysia, from 78.57% to 65.44% between the years 1990 to 2010. Similarly, Sarkar *et al.*, (2021) observed a forest cover change of approx. 21598 hectares in southern part of Jangalmahal, West Bengal, India between the year 2000 to 2020 using the NDVI change matrix.

**Land Surface Temperature (LST)**

LST can be another environmental component influenced by forest cover change because variation in surface temperature impacts the conditions like deforestation, evapotranspiration, droughts, etc. LST is influenced by factors such as surface roughness, wind speed, and surface conductance, also by the availability of water for evapotranspiration and the amount of shortwave radiation absorbed by the surface which is known as surface albedo. Since tree roots are usually deeper and have access to more water resources, landscapes with healthy vegetation cover are likely to have higher rates of evapotranspiration and hence lower LSTs (Van Leeuwen *et al.*, 2011). Entezari *et al.* (2016) verified the direct effects of vegetation loss, drought conditions, dryness, and deforestation on the rising LST, and as per Peng *et al.*, (2014) afforestation and greenery lowers the local land surface temperatures. Similarly, Tepanosyan *et al.*, (2021) observed that green and built-up regions have a substantial influence on LST variation with an inverse relationship between increased vegetation cover and decreased LST and vice versa. Sinha *et al.*, (2014) assessed the spectral radiance and surface emissivity values obtained from NDVI for a moist deciduous tropical forest area of the Munger forests (Bihar, India) for LST estimation and concluded that temperature was lowest in areas covered with vegetation whereas built-up area, barren land, and exposed territory had a greater LST value. Khorrami *et al.*, (2019) conducted a regression analysis and found a high correlation (0.98) between deforestation and spatial rise in land surface temperature. Soil moisture in three talukas of Panchmahal district, Gujarat State was estimated using Sentinel-1 C-band SAR and Landsat-8 OLI data where LST was estimated using Landsat-8 thermal data (Sutaria *et al.*, 2021).

**Urban Thermal Field Variance Index (UTFVI)**

Elevated LST causes the Surface Urban Heat Island (SUHI) effect, which worsens the meteorological condition and the vulnerability of the SUHI effect can be quantified by using Urban Thermal Field Variance Index

(UTFVI) (Naim and Kafy, 2021). Using the UTFVI ecological evaluation classification map, (Liu and Zhang, (2011) discovered that uninhabited areas have relatively high vegetation cover and an excellent ecological evaluation index, whereas intensive urban development leads to a deteriorated eco-environment with the worst ecological evaluation index. According to Faisal *et al.*, (2021), the optimal thermal state for living is none, with a weak effect on UTFVI, whereas the strongest zone reflects a vulnerable environment receptive to increased UHI phenomena. Since the significant increase in the LST and UTFVI has a direct impact on the environmental consequences, present study was intended to analyze the current and historical status of forest cover and LST values as well as the potential linkage between Land Surface Temperature, Urban Thermal Field Variance Index, and deforestation/ afforestation processes.

**Data used**

*Remote Sensing Satellite Data*

In this study, multi-temporal Landsat digital data of Landsat-5 Thematic Mapper (TM), Landsat-8 Operational Land Imager (OLI), and Sentinel-2 MSI data for the years from 1991 to 2021 covering the study area of Pavagadh in Gujarat State was downloaded from the website <https://earthexplorer.usgs.gov/>.

Table 1. Acquired Landsat and Sentinel-2 Multispectral Data Specifications

Sr. No	Satellite / Sensor	Spatial Resolution (m)	Path /Row	Acquisition Date
1	Landsat-5/ TM	30	148/045	23-Jan-1991
2	Landsat-5/ TM	30	148/045	10-Jan-2001
3	Landsat-5/ TM	30	148/045	14-Jan-2011
4	Landsat-8/ OLI TIRS	30	148/045	26-Feb-2021
5	Sentinel-2 (MSI)	10		17-Jan-2021

*Field Data Collection*

The field data related to forest cover, forest density, and status of other vegetation and crops in the study area were collected during January 2021. The sample points for field data collection in the study area were selected based on the visual interpretation of Landsat data of Jan-2021. The GPS measurements of selected sites along with field photographs were also corrected for accurate location of these field data on the Satellite data. Some of the field photographs of forest cover in the study area are given in Figure 2.

**Remote Sensing Satellite Data Analysis**

The Landsat and Sentinel-2 multi-spectral and multi-temporal data covering the study area were analyzed using the following major steps:

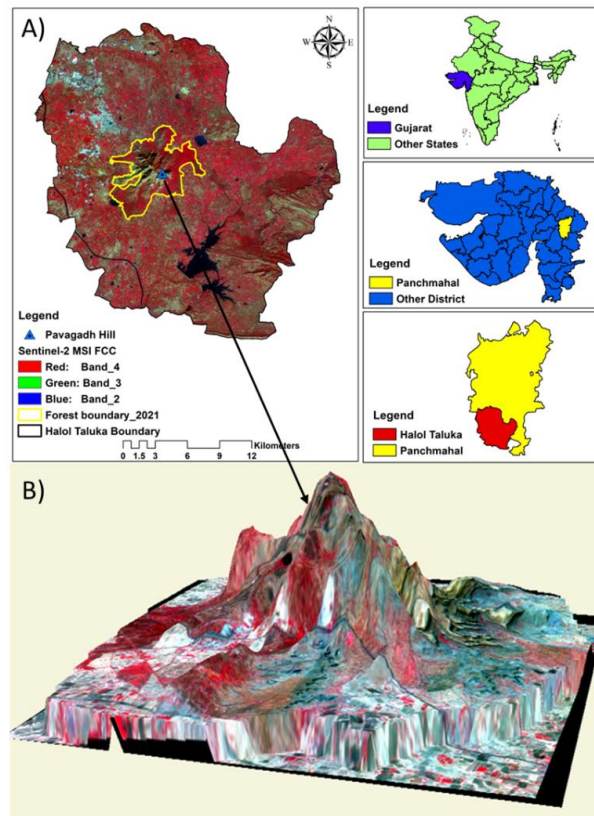


Fig. 1. Location Map (A) and DEM image of the study area (B)



Fig. 2. Forest Features of Study Area

**Geo-referencing of Landsat Data**

The Landsat TM and OLI and Sentinel-2 MSI data used in this study are ortho-rectified products. They are basically in the World Geodetic System (WGS-84) datum and the Universal Transverse Mercator (UTM) projection system. Landsat images were geo-referenced using base maps of the study area. Landsat Sentinel-2 images were georeferenced into the UTM projection (UTM/ Zone 42 North), through the image to map georeferencing and other images were georeferenced using image-to-image registration. A sufficient number of well-distributed ground control points (GCPs) were selected and a second-order polynomial transformation model with nearest-neighbour image resampling was applied. The overall accuracy of the transformation for most of the images was

between 0.45 to 0.75 pixels. Landsat satellite images of 1991, 2001, 2011, and 2021 were interpreted to map and monitor the changes in forest cover over the last 30 years in the Pavagadh area in Gujarat state.

**Land Surface Temperature Estimation**

The Landsat-8 OLI and TIRS digital data were analyzed for the estimation of the Land Surface Temperature (LST) of the study area. The procedure adopted by Sutaria *et al.*, 2021 was followed in this study. Thermal infrared sensor Band-10 data and operational land imager Band-4 and Band-5 data were used in estimating LST and characteristics of these bands (Department of the Interior U.S. Geological Survey, 2016) shown in Table 2.

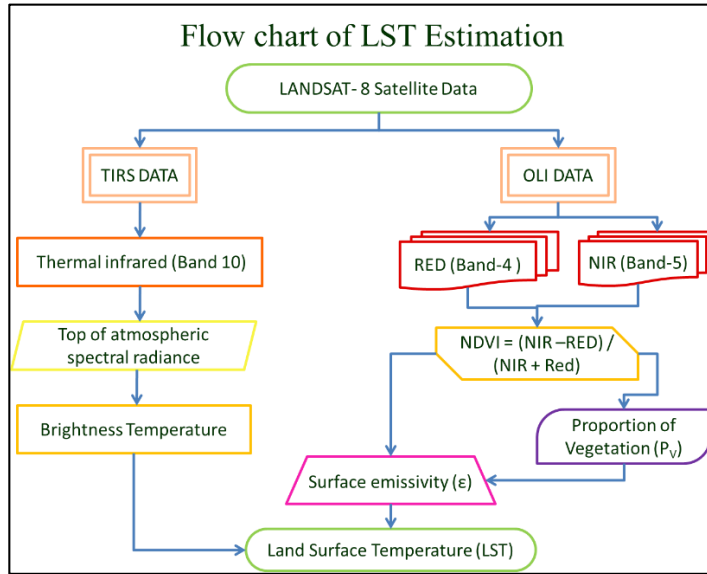


Fig. 3. Procedure adopted for LST estimation using Landsat-8 data

Table 2. Spectral Band characteristics of LANDSAT-8

Band	Resolution (m)	Spectral Band	Wavelength(μm)	Solar irradiance (W/(m <sup>2</sup> μm))
4	30	Red	0.630 - 0.680	1574
5	30	Near Infrared	0.845 - 0.885	955
10	30	Longwave Infrared	10.60 - 11.19	--

From the Landsat-8 digital data; Red, NIR, and TIRS bands were used for the calculation of LST, and steps described by Avdan and Jovanovska, 2016 were followed in this study. The major steps are:

Proceeding with the conversion of digital numbers to top-of-the-atmosphere radiance values and then to at- Figure 2. Field photographs with GPS coordinate on satellite data sensor brightness temperature. The following step is to compute the NDVI and vegetation proportion. Surface emissivity is calculated further utilizing an empirical relationship based on the NDVI. Eventually, LST is calculated using the simplified Plank's law. The flow chart of LST estimation is given in Figure 3.

*Top of atmospheric spectral radiance*

In the first step of LST estimation, band 10 from Landsat-8 OLI data has been used for the estimation of top of atmospheric (TOA) spectral radiance (Lλ), (Omar and Kumar, 2021):

$$L\lambda = M_1 \times Q_{cal} + A_1 - Q_i \quad (Eq.1)$$

Where,  
 Lλ= Top of atmospheric spectral radiance,  
 M<sub>1</sub>= Band-specific multiplicative rescaling factor,  
 Q<sub>cal</sub> = Band-10 image,  
 A<sub>1</sub>= Band-specific additive rescaling factor,  
 Q<sub>i</sub>= correction for Band 10

*Conversion of Radiance to At-Sensor Temperature*

Utilizing the thermal constants provided in the Landsat-8 metadata file, the brightness temperature is estimated by converting radiance to at-sensor temperature:

$$BT = \frac{K_2}{\ln(K_1/L\lambda) + 1} - 273.15 \quad (Eq. 2)$$

Where, BT= Brightness temperature, K<sub>1</sub> and K<sub>2</sub>= Band-specific thermal constants,  
 Lλ= Top of atmospheric spectral radiance

*NDVI for Emissivity Correction*

NDVI can be used to estimate the general condition of the vegetation as well as estimate the amount of vegetation that is present (Rouse et al., 1974; Weng et al., 2004). The NDVI is essential for estimating the Proportion of Vegetation (PV):

$$NDVI = \frac{NIR(band 5) - R(band 4)}{NIR(band 5) + R(band 4)} \quad (Eq.3)$$

Where,  
 NDVI= Normalized Difference Vegetation Index  
 NIR = Near-infrared band (Band-5),  
 R = Red band (Band-4)

*2.4.4 Calculating the Proportion of Vegetation*

$$P_v = \left( \frac{NDVI - NDVI_s}{NDVI_v - NDVI_s} \right)^2 \quad (Eq.4)$$

Where,  
 P<sub>v</sub> = Proportion of Vegetation, NDVI= Normal Difference Vegetation Index, NDVI<sub>v</sub> = 0.5, NDVI<sub>s</sub> = 0.2

*Calculating Land Surface Emissivity (LSE)*

To calculate the LSE, the water category has been classified with an emissivity value of 0.991 and also with an NDVI value of less than 0. For the calculation of soil, values of NDVI between 0 and 0.2 and the emissivity



value of 0.996 has been taken into account. And the same way, NDVI value greater than 0.5 and 0.973 emissivities has been considered as vegetation. It is considered to be covered with vegetation, and the value of 0.973 is assigned. Finally, to calculate the LSE using the formula (5), NDVI values between 0.2 and 0.5 have been taken into account.

$$\epsilon_{\lambda} = \epsilon_{v\lambda}P_v + \epsilon_{s\lambda}(1 - P_v) + C_{\lambda} \quad (\text{Eq.5})$$

Where,

$\epsilon_{\lambda}$  =Land Surface Emissivity,  $P_v$  =Proportion of Vegetation,  $\epsilon_{v\lambda} = 0.973$ ,  $\epsilon_{s\lambda} = 0.996$ ,  $C_{\lambda}$  =Surface roughness (0.005)

**Land surface temperature Computation**

Bendib et al. (2017) recommended that band 10 of TIRS of Landsat 8 can be used as a single spectral band for the estimation of land surface temperature. The following equation is used to calculate land surface temperature (LST):

$$T_s = \frac{BT}{\left\{1 + \left[\frac{\lambda BT}{\rho}\right] \ln \epsilon_{\lambda}\right\}} \quad (\text{Eq.6})$$

Where,

$T_s$  represents Land surface temperature (°C),  $BT$  shows Brightness temperature, whereas  $\epsilon_{\lambda}$  indicates Land Surface Emissivity and  $\lambda$  refers to limiting wavelength (10.895), while  $\rho$  is  $1.438 \times 10^{-2}$  m.

**Urban Thermal Field Variance Index**

$$\text{UTFVI} = \frac{T_s - T_{\text{mean}}}{T_s} \quad (\text{Eq.7})$$

Where,  $T_s$  is the LST of a pixel (°C), and  $T_{\text{mean}}$  is the mean LST of the whole study area (°C). The UTFVI was calculated for the years 1991 and 2021. It helps to evaluate the influence of the Urban Heat Island and can be separated into six stages with six particular ecological evaluation indices to know the ecological condition of that particular area. (Renard et al., 2019).

Table 3. Threshold values of UTFVI and ecological evaluation index (Liu and Zhang, 2011)

Urban Thermal Field Variation Index	Urban Heat Island Phenomenon	Ecological Evaluation Index
< 0.0	None	Excellent
0.0 - 0.005	Weak	Good
0.005 - 0.010	Middle	Normal
0.010 - 0.015	Strong	Bad
0.015 - 0.020	Stronger	Worse
> 0.020	Strongest	Worst

**Results and Discussion**

**Spatio-temporal Forest Cover Changes based on NDVI**

Vegetation indices have been used in remote sensing to track temporal changes in vegetation for many years. In the present study, NDVI images of the study area were generated for the years 1991, 2001, 2011 and 2021. The

NDVI values slightly higher than zero indicate the presence of vegetation classes. The NDVI values in this study higher than 0.22 indicated moderate vegetation while NDVI values higher than 0.35 indicated healthy and dense vegetation. Only active vegetation has a positive NDVI, with values typically ranging from 0.1 to 0.6 at the higher end of the range, suggesting enhanced photosynthetic activity and canopy density (Tarpley et al., 1984). The NDVI thresholding method was adopted to categorize forest classes into four major classes like dense forest vegetation, moderate forest vegetation, sparse forest vegetation and other land use class. The results indicated that NDVI values were significantly different during the period of 3-decades from 1991 to 2021. The changes in forest density classes were monitored by studying the changes in NDVI values of different forest density classes. The comparison of changes in NDVI values based on forest density classes is given in Figure 4(a, b, c, d).

Table 4. Area under Forest Density classes from 1991 to 2021

NDVI Class	Area under Different Forest Classes (km <sup>2</sup> )			
	1991	2001	2011	2021
Dense Forest Vegetation	2.041	1.904	5.144	7.195
Moderate Forest Vegetation	1.920	4.273	4.997	5.098
Sparse Forest Vegetation	7.718	12.234	9.708	11.127
<b>Total Forest Area</b>	<b>11.679</b>	<b>18.411</b>	<b>19.849</b>	<b>23.420</b>
Other Land Use	27.824	18.879	16.930	12.899

Table 4 indicates that the total estimated forest cover area has gradually increased from 1991 to 2021 and the total forest area has doubled during this period of 30 years. The forest cover was 11.68 km<sup>2</sup>, 18.41 km<sup>2</sup>, 19.85 km<sup>2</sup>, and 23.42 km<sup>2</sup>, during 1991, 2001, 2011, and 2021, respectively. There is a significant increase in sparse forest vegetation, which indicates that there is a large amount of forest plantation activity in the study area was undertaken by the Forest department. There has been a growth of approximately 5.15 km<sup>2</sup> in densely healthy forest vegetation cover from 1991 to 2021. Simultaneously, there was an upsurge in moderate and sparse vegetation.

**Land Surface Temperature Mapping**

The LST maps were generated to study the impact of forest vegetation cover on the LST changes in the research area. The spatial distribution of LST changes during the last three decades was monitored. LST distribution maps of 1991 and 2021 are given in Figure 5 (a) and (b), respectively.

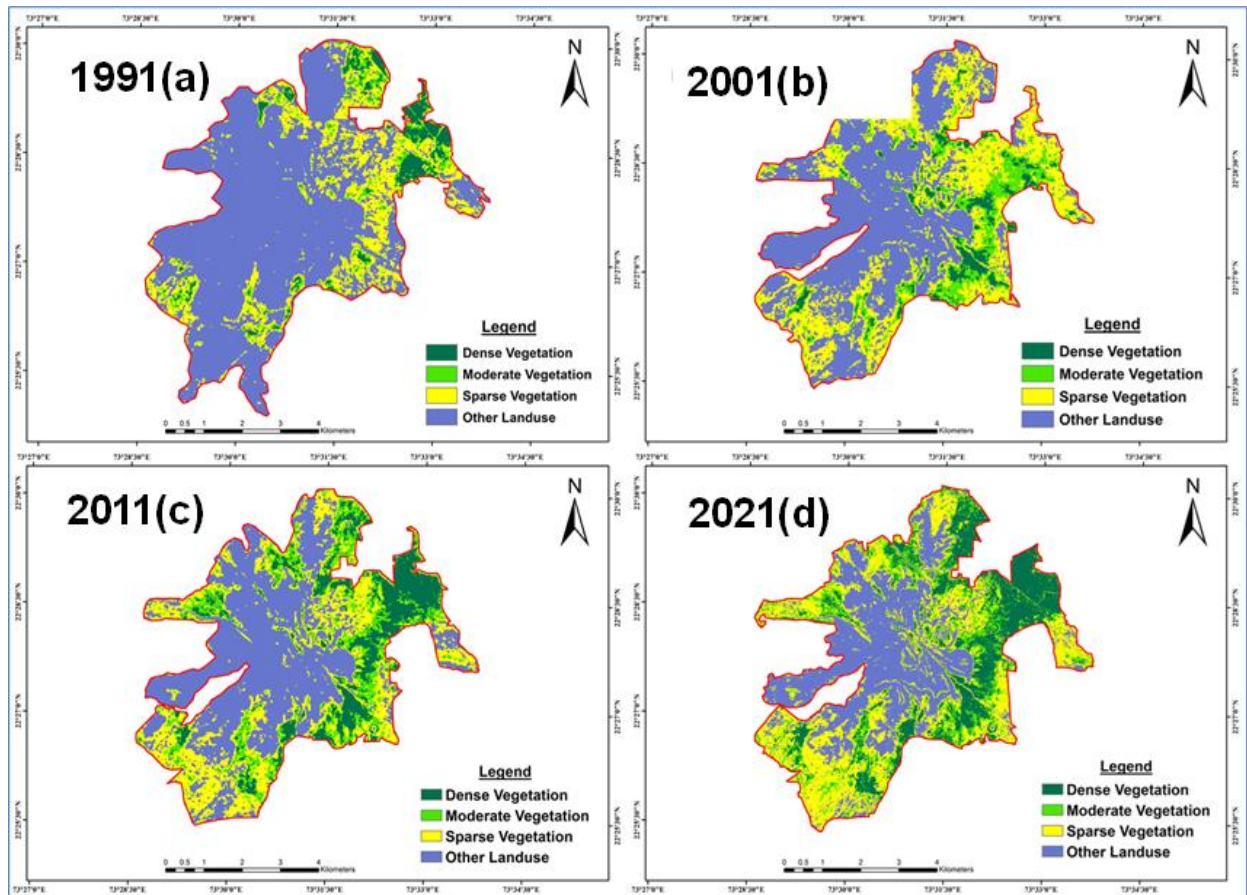


Fig. 4. NDVI derived classified map of the study area for 1991 (a), 2001 (b), 2011 (c) and 2021(d)

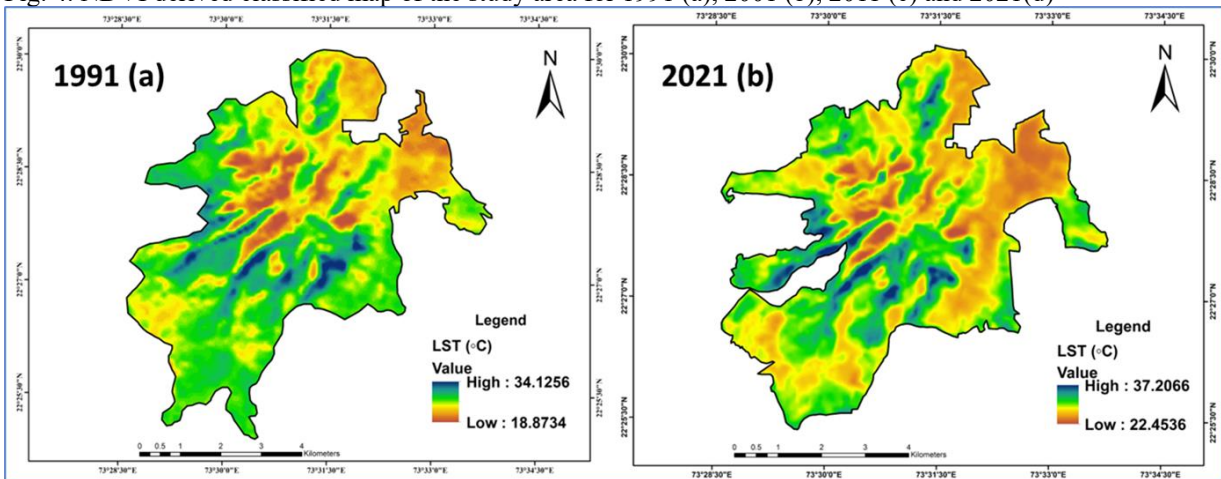


Fig5. Land Surface Temperature maps of the years 1991 (a) and 2021 (b)

The minimum and maximum temperatures in 1991 were 18.87 and 34.12 °C, respectively. Whereas in the year 2021 land surface temperatures increased by almost 3-4 °C in comparison to 1991 in the study area. The minimum temperature was around 22.45 °C and the maximum temperature was 37.20 °C in 2021. However, the LST distribution map indicates that the Increased temperature is mostly distributed over the central and western parts of the study area where the mountainous terrain exists. The comparative study of NDVI and LST images indicates that the increase in LST is observed in the areas where NDVI values are very low indicative of poor vegetation

cover. These results bring out a significant fact that in the areas where moderate and dense forest cover is present, the LST was lower as compared to areas with poor vegetation cover in the study area. This indicates that there is an inverse relationship between forest cover distribution and LST.

#### **Urban Thermal Field Variance Index Monitoring**

The Urban Thermal Field Variance Index images for different years were generated and analyzed for monitoring the changes in the study area. The UTFVI images of 1991 and 2021 are given in Figure 6 (a) and (b).

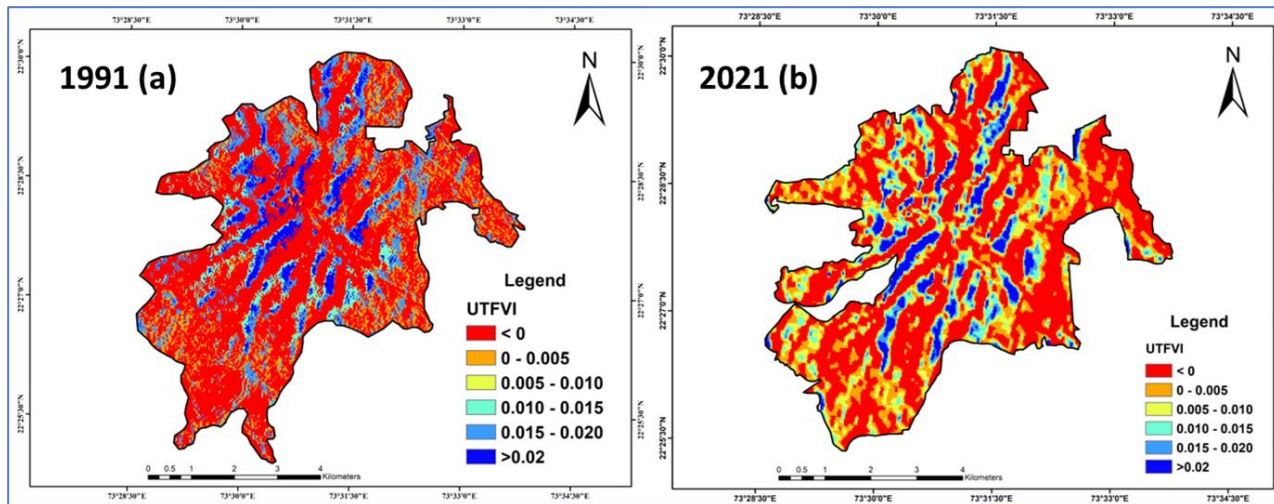


Fig. 6. Urban thermal field variance index classification map with Ecological evaluation of the years 1991(a) & 2021(b)

Table 5. UTFVI and ecological evaluation index of the years 1991 and 2021

Urban Thermal Field Variation Index	Urban Heat Island Phenomenon	Ecological Evaluation Index	Area (km <sup>2</sup> )	
			1991	2021
<0	None	Excellent	24.57	18.25
0.0 - 0.005	Weak	Good	5.27	7.11
0.005-0.010	Middle	Normal	-	4.65
0.010-0.015	Strong	Bad	2.18	2.69
0.015-0.020	Stronger	Worse	5.11	1.49
>0.020	Strongest	Worst	2.38	2.10

A comparison of the obtained UTFVI threshold values and the Urban Heat Island Phenomena with the ecological evaluation index of the study area for the years 1991 and 2021 reveals that the area covered in the Ecological Evaluation Index excellent category and having UTFVI value (<0) condition in 1991 was 24.56 km<sup>2</sup>, while it gets deteriorated to 18.25 km<sup>2</sup> in 2021. The results of this comparison show that there has been a decline in the health of forest cover vegetation over time (Table 5). UTFVI values of 0.015-0.020 suggest a stronger urban heat island phenomenon in conjunction with a worsening ecological state of the land. Around 5 km<sup>2</sup> of land was covered in strongly worse ecological conditions in 1991, however, this was decreased to 1.5 km<sup>2</sup> by 2021. But the urban development leads to a degraded eco-environment with the worst (> 0.020) ecological evaluation index. However, the ecological evaluation index reveals that the vegetative quality is gradually improving to normal conditions in reference to the year 1991.

**Conclusion**

In this research, the variation in LST, NDVI, UTFVI, and the ecological assessment index was used to assess the change in forest cover patterns during the previous three decades in terms of temporal and spatial variations in land cover and surface temperatures. The Landsat and Sentinel-2 MSI data of 1991, 2001, 2011, and 2021 were analyzed for monitoring changes in forest cover throughout 30 years. Since forests include a diverse range of plants and trees, proper forest management and conservation help to maintain healthy vegetation. As

some of the significant environmental phenomena could be deduced from climatic variables on the earth's surface, tracking LST, NDVI, and UTFVI variations appears to be crucial in any environmental protection effort. The major conclusions of this study are as follows:

- ❖ The results indicated that the total forest cover area has gradually increased from 1991 to 2021 and the total forest area has doubled during this period of 30 years.
- ❖ The LST analysis indicates that land surface temperatures have increased by almost 3- 4 °C during 2021 as compared to 1991 in the study area.
- ❖ The comparative study of NDVI and LST images indicates that the increase in LST is observed in the areas where NDVI values are very low indicative of poor vegetation. This indicates that there is an inverse relationship between forest cover distribution and LST.
- ❖ A comparison of the obtained UTFVI threshold values and the Urban Heat Island Phenomena with the ecological evaluation index of the study area for the years 1991 and 2021 reveals that the area covered in the Ecological Evaluation Index excellent category and having UTFVI value (<0) condition has decreased over the years.

Based on the results obtained, it can be concluded that the healthy vegetation in the form of green areas offered vital

and considerable contributions to the regulation of land surface temperature, as healthy vegetation increases, it potentially lowers the land surface temperature of that particular area with excellent ecological health conditions.

### Acknowledgments

The authors express their sincere thanks to the Director General (DG), Bhaskaracharya Institute for Space Applications and Geo-informatics (BISAG-N), Ministry of Electronics and Information Technology (MEITY), Government of India, for his keen interest and valuable guidance to carry out this study. The satellite data was downloaded from the United States Geological Survey is thankfully acknowledged. The authors would like to thank the editor and anonymous reviewers for their insightful and constructive comments to improve the original manuscript.

### References

- Aburas, M. M., Abdullah, S. H., Ramli, M. F., Ashaari, Z. H. (2015). Measuring Land Cover Change in Seremban, Malaysia Using NDVI Index. *Procedia Environmental Sciences*, 30, 238–243. <https://doi.org/10.1016/j.proenv.2015.10.043>
- Anand, A., Singh, S. K., Kanga, S. (2018). Estimating the change in forest cover density and predicting NDVI for west Singhbhum using linear regression. *Int. J. Environ. Rehabil. Conserv*, 9, 193-203. <https://doi.org/10.31786/09756272.18.9.1.125>
- Artis, D. A., Carnahan, W. H. (1982). Survey of emissivity variability in thermography of urban areas. *Remote sensing of Environment*, 12(4), 313-329.
- Avdan, U., Jovanovska, G. (2016). Algorithm for automated mapping of land surface temperature using LANDSAT 8 satellite data. *Journal of sensors*, 2016.
- Bendib, A., Dridi, H., Kalla, M. I. (2017). Contribution of Landsat 8 data for the estimation of land surface temperature in Batna city, Eastern Algeria. *Geocarto International*, 32(5), 503–513. <https://doi.org/10.1080/10106049.2016.1156167>
- Chandrasekar, K. (2016). Geo-spatial meteorological products for Agricultural drought assessment. *NRSC User Interaction Meet- PPT*.
- Entezari, A., Amir Ahmadi, A., Aliabadi, K., Khosravian, M., Ebrahimi, M. (2016). Monitoring Land Surface Temperature and Evaluating Change Detection Land Use (Case Study: Parishan Lake Basin). *Hydrogeomorphology*, 2(8), 113-139.
- Esetlili, M. T., Bektas Balcik, F., Balik Sanli, F., Kalkan, K., Ustuner, M., Goksel, C., Gazioğlu, C. Kurucu, Y. (2018). Comparison of Object and Pixel-Based Classifications For Mapping Crops Using Rapideye Imagery: A Case Study Of Menemen Plain, Turkey. *International Journal of Environment and Geoinformatics*, 5(2), 231-243. <https://doi.org/10.30897/ijegeo.442002>
- Faisal, A. Al, Kafy, A. Al., Al Rakib, A., Akter, K. S., Jahir, D. M. A., Sikdar, M. S., Ashrafi, T. J., Mallik, S., Rahman, M. M. (2021). Assessing and predicting land use/land cover, land surface temperature and urban thermal field variance index using Landsat imagery for Dhaka Metropolitan area. *Environmental Challenges*, 4, 100192. <https://doi.org/10.1016/j.envc.2021.100192>
- Forkuo, E. K., Frimpong, A. (2012). Analysis of forest cover change detection. *International journal of remote sensing applications*, 2(4), 82-92. <https://www.researchgate.net/publication/269222395>
- Khorrami, B., Gunduz, O., Patel, N., Ghoulzlane, S., Najjar, M. (2019). Land surface temperature anomalies in response to changes in forest cover. *International Journal of Engineering and Geosciences*, 4(3), 149-156. <https://doi.org/10.26833/ijeg.549944>
- Liu, L., Zhang, Y. (2011). Urban heat island analysis using the Landsat TM data and ASTER data: A case study in Hong Kong. *Remote sensing*, 3(7), 1535-1552. <https://doi.org/10.3390/rs3071535>
- Malik, M. M., Tali, J. A., Nusrath, A. (2017). Spatio-Temporal Changes of Forest Cover in Baramulla District. *Journal of Remote Sensing & GIS*, 8(3).
- Markham, B. L., Barker, J. L. (1985). Spectral characterization of the Landsat Thematic Mapper sensors. *International Journal of Remote Sensing*, 6(5), 697-716.
- Naim, M. N. H., Kafy, A. A. (2021). Assessment of urban thermal field variance index and defining the relationship between land cover and surface temperature in Chattogram city: A remote sensing and statistical approach. *Environmental Challenges*, 4(April), 100107.
- Nath, B. (2014). Quantitative Assessment of Forest Cover Change of a Part of Bandarban Hill Tracts Using NDVI Techniques. *Journal of Geosciences and Geomatics*, 2(1), 21–27. <https://doi.org/10.12691/jgg-2-1-4>
- Omar, P. J., Kumar, V. (2021). Land surface temperature retrieval from TIRS data and its relationship with land surface indices. *Arabian Journal of Geosciences*, 14(18), 1-14.
- Peng, S. S., Piao, S., Zeng, Z., Ciais, P., Zhou, L., Li, L. Z., ... Zeng, H. (2014). Afforestation in China cools local land surface temperature. *Proceedings of the National Academy of Sciences*, 111(8), 2915-2919.
- Renard, F., Alonso, L., Fitts, Y., Hadjiosif, A., Comby, J. (2019). Evaluation of the effect of urban redevelopment on surface urban heat islands. *Remote Sensing*, 11(3). <https://doi.org/10.3390/rs11030299>
- Rouse Jr, J. W., Haas, R. H., Schell, J. A., Deering, D. W. (1973). Monitoring the vernal advancement and retrogradation (green wave effect) of natural vegetation (No. NASA-CR-132982).
- Sarkar, S., Bandyopadhyay, J., Giri, S. (2021). Spatio-Temporal analysis of forest conversion in contrasting LULC and vegetation extraction using spatial information southern part of Jangalmahal, West Bengal, India. *Int J Appl Res* 2021;7(4):247-254. DOI: 10.22271/allresearch.2021.v7.i4d.8501
- Sinha, S., Pandey, P. C., Sharma, L. K., Nathawat, M. S., Kumar, P., Kanga, S. (2014). Remote estimation of land surface temperature for different LULC features of a moist deciduous tropical forest region. *Remote*



sensing applications in environmental research, 57-68.

- Sutariya, S., Hirapara, A., Meherbanali, M., Tiwari, M., Singh, V. Kalubarme, M. (2021). Soil Moisture Estimation using Sentinel-1 SAR Data and Land Surface Temperature in Panchmahal District, Gujarat State. *International Journal of Environment and Geoinformatics*, 8(1), 65-77. <https://doi.org/10.30897/ijegeo.777434>
- Tarpley, J. D., Schneider, S. R., Money, R. L. (1984). Global vegetation indices from the NOAA-7 meteorological satellite. *Journal of Climate and Applied Meteorology*, 491-494.
- Tepanosyan, G., Muradyan, V., Hovsepyan, A., Pinigin, G., Medvedev, A., Asmaryan, S. (2021). Studying spatial-temporal changes and relationship of land cover and surface Urban Heat Island derived through remote sensing in Yerevan, Armenia. *Building and Environment*, 187, 107390.
- van Leeuwen, T. T., Frank, A. J., Jin, Y., Smyth, P., Goulden, M. L., van der Werf, G. R., Randerson, J. T. (2011). Optimal use of land surface temperature data to detect changes in tropical forest cover. *Journal of Geophysical Research: Biogeosciences*, 116(G2). <https://doi.org/10.1029/2010JG001488>
- Weng, Q., Lu, D., Schubring, J. (2004). Estimation of land surface temperature-vegetation abundance relationship for urban heat island studies. *Remote sensing of Environment*, 89(4), 467-483.
- Yismaw, A., Gedif, B., Addisu, S., Zewudu, F. (2014). Forest cover change detection using remote sensing and GIS in Banja district, Amhara region, Ethiopia. *International Journal of Environmental Monitoring and Analysis*, 2(6), 354.